MODELLING THE MAGNETIC DISTURBANCES DUE TO ROAD-TRAFFIC

J.-J. Schott and A. Chambodut [*]

Department of Magnetic Observatories; Université de Strasbourg/EOST, CNRS UMR 7516; 5 rue Rene Descartes 67084 Strasbourg Cedex, France.
**Email :* aude@unistra.fr

ABSTRACT

Magnetic disturbances due to the traffic are tentatively modelled assuming that the sources are moving dipoles. The influencing section of the road ("useful" portion) should be modelled in 3D. The parameters of the model (time of closest position to the magnetometer, velocity, including its sign, dipole moment) are fairly accurately estimated. The fit is improved with the incorporation of a small induction effect.

1 INTRODUCTION

Disturbances due to human activities are a major concern for magnetic observatories and, in the past, scientists were obliged to move many of the observatories away from disturbing sources. This problem is enhanced by the worldwide tendency to extend records to higher frequencies. Specific examples are to be found in recent literature, for instance Clark et al. (1994), Hejda and Horacek (2001), and Okawa et al. (2007). The last example is closely connected to the one discussed here, in so far as it deals with disturbances due to traffic close to the observatory. The example discussed herein is taken from a geophysical station, named Welschbruch, located in the Vosges mountains, France, where the Earth's magnetic is nearly permanently recorded according to current standards. In our example, the disturbance due to the traffic on the road that passes nearby is nearly smoothed out on one minute data but is clearly identified on the one second records. The aim of the study reported herein is the modelling of this disturbance, based upon a fairly accurate survey of the section of interest of the road, using GPS measurements, on one hand, and the assumption that the magnetic field produced by the passing vehicles may be approximated by a moving dipole, on the other hand.

2 WELSCHBRUCH STATION : 3D ROAD MODEL

Welschbruch geophysical station is located in the Vosges mountains, about 40 km south of Strasbourg, France. It is equipped like a standard magnetic observatory and serves mainly to testing instruments and training observers yearly. The acquisition system was recently upgraded to one second sampling rate with the device built up at EOST, Strasbourg (Fotzé et al., 2007).

Figure 1 shows the position of the variometer house (V), the absolute house (A), and of the road. The shape of the road has been sampled with GPS measurements, along the downhill side of the road, the spacing ranging from 5 to 20 m, according to the curvature of the path. The corresponding curvilinear abscissae have been measured by means of a tape line deployed along the same downhill side. The origin is the point (P) closest to the variometer, and the orientation is positive downwards. Two sets of points, one for the downhill and one for the uphill lane, have been derived from the sampled points and interpolated with a smoothing cubic spline. Figure 2 displays the shape of the two lanes in the geographical reference frame centered on the magnetometer location.

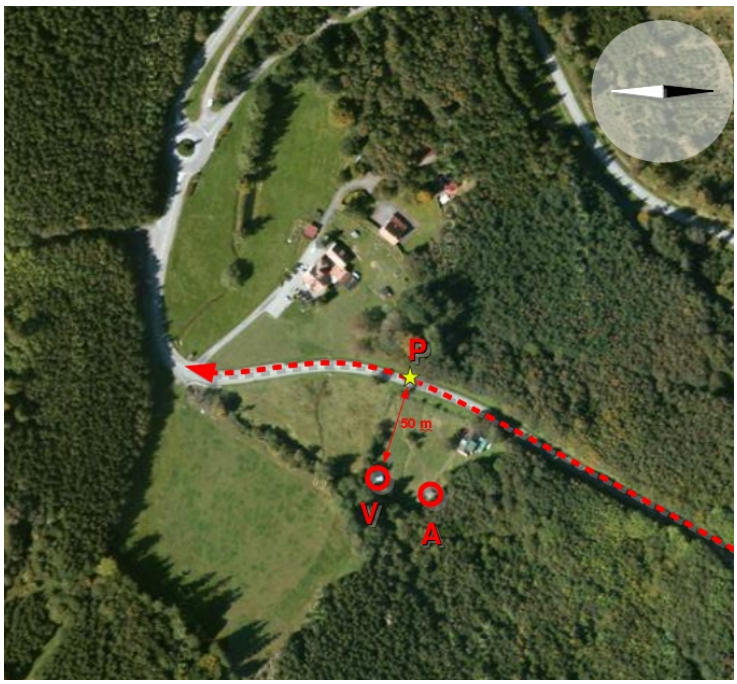

Figure 1. Welschbruch geophysical station (Vosges, Eastern France), lat. 48° 25' N / lon. 7°21' E

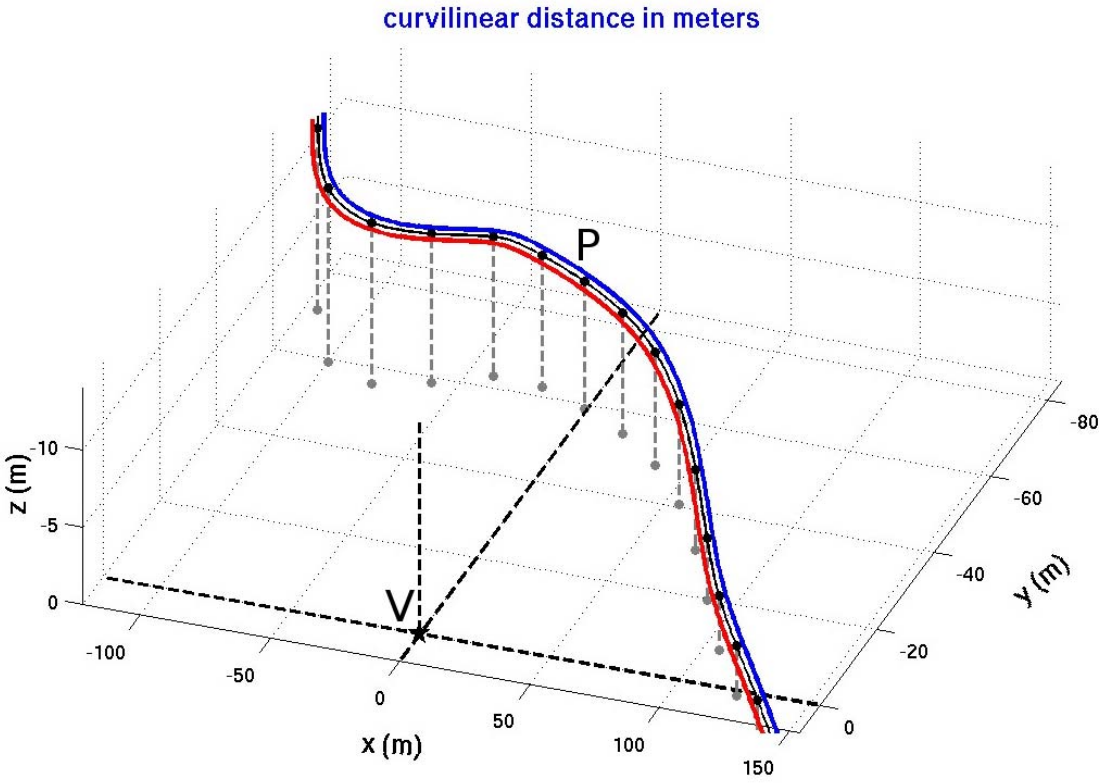

Figure 2. The 3D road model. Red curve: downhill lane. Blue curve: uphill lane. Dotted lines are the axes of the geographical reference frame, X northwards, Y eastwards, Z vertical downwards. The origin coincides with the location of the magnetometer.

The separation between the two lanes is large enough to give rise to two distinguishable signals on the magnetometer which are about 50m apart (see Figures 3 and 4).

3 MODELLING A MOVING DIPOLE

The magnetic effect of the vehicles has been approximated by a moving dipole M . The disturbance field $S_p = (X_p, Y_p, Z_p)$ is expressed in the geographical reference frame by:

$$S_p = \mathrm{A} \cdot M \tag{1}$$

Where :

$$A = \frac{\mu_0}{4\pi r^5}\begin{bmatrix} 2X^2 - Y^2 - Z^2 & 3XY & 3XZ \\ 3XY & 2Y^2 - X^2 - Z^2 & 3YZ \\ 3XZ & 3YZ & 2Z^2 - X^2 - Y^2 \end{bmatrix} \tag{2}$$

(X,Y,Z) give the position of the dipole equivalent to the moving vehicle. X, Y, Z are functions of the curvilinear abscissa s , and $r = (X^2 + Y^2 + Z^2)^{1/2}$. As mentioned above, $X(s)$, $Y(s)$, $Z(s)$ are approximated by smoothing cubic splines depending on the uphill or downhill direction. Figure 3 shows the shape of the three components of the disturbance signal as a function of s , the source being a dipole approximately parallel to the Earth's field ($D = 0°, I = 63°$) and strengh $M = 2.10^4\ A.m^2$. Of course, as expected, the magnitude is slightly larger for a downhill moving vehicle, which is a little bit closer to the magnetometer.

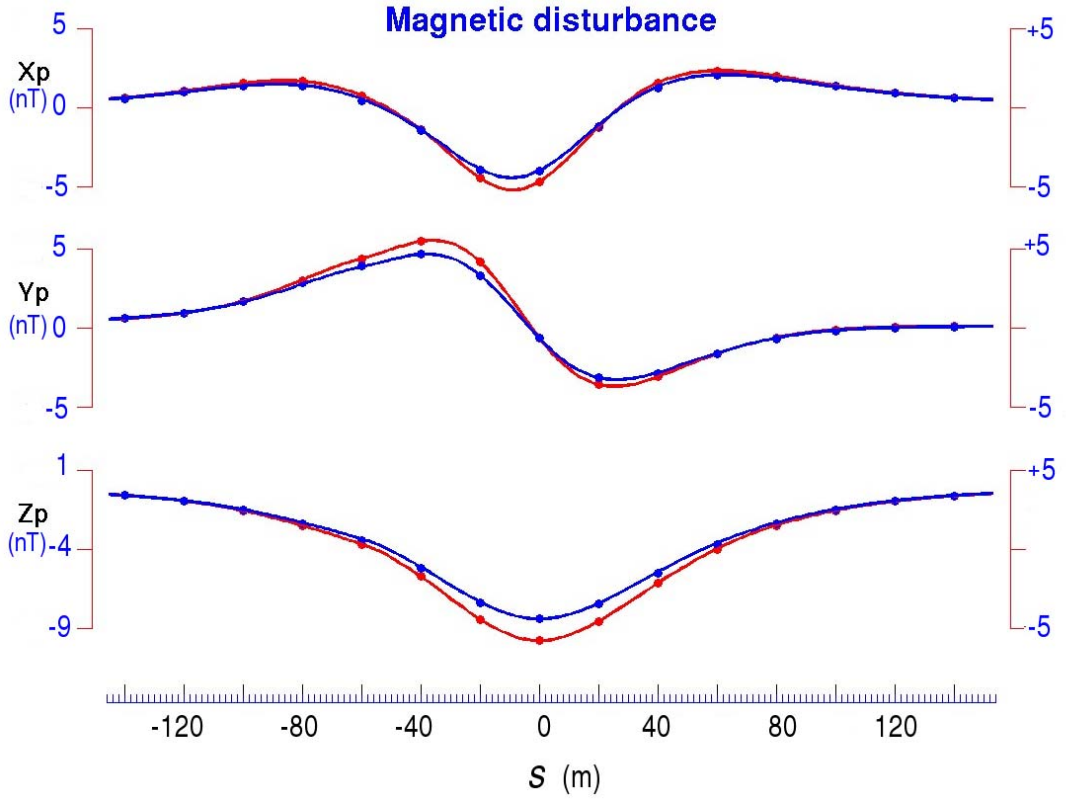

Figure 3. Modelled disturbance field produced by a vehicle moving downhill (red curves) or uphill (blue curves) with respect to curvilinear abscissa.

If the independent variable is now time instead of s , the velocity of the vehicle appears to be a key parameter for the shape of the disturbance. We have assumed a constant velocity along the trajectory, which is clearly an oversimplification: obviously, the vehicles slow down in the curve upwards and generally accelerate in the straight section. Thus, a distortion of the modelled signal is to be expected. Under the assumption of constant velocity, the relation between time and s is merely:

$$s(t) = v(t - t_o)$$

where t_o is the time of the position closest to the magnetometer. v is the velocity, with positive (resp. negative) sign for downhill (resp. uphill) movement. On Figure 4, "warm" colors are for uphill movements whereas "cold" colors are for downhill movements. d is the distance to the magnetometer. Note that

X_p and Z_p disturbances are symetric with respect to $s = 0$ whereas Y_p is antisymetric. The clear distinction in Y_p signal between positive and negative speeds allows discrimination among vehicles moving downhill and uphill. Note the abrupt drop towards 0 for high speeds. It turns out that for these speeds, $s(t)$ is outside the limits of the sampled portion of the road. We have merely set the signal to 0 for these ranges. This slight distortion is not a serious drawback for the estimation of the parameters of the model.

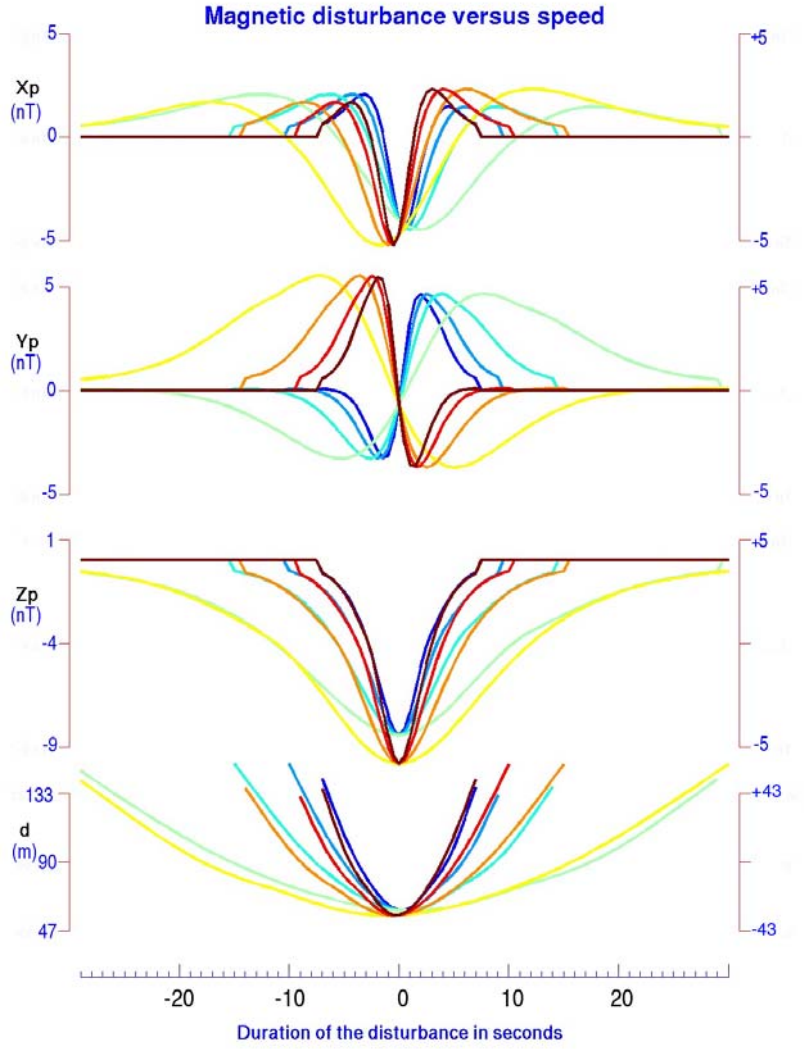

Figure 4. Modelled disturbance field at the location of the variometer produced by a uphill moving vehicle (warm colors) and an downhill moving one (cold colors) with respect to time.

4 DISTURBANCE MODELLING

Figure 5 shows an example of an isolated, clearly identified disturbance, recorded by the triaxial magnetometer as well as by a scalar magnetometer. The duration of the disturbance is about 20s. The sampling rate of the scalar magnetometer being only 10s, this record will not been used further. (X_v, Y_v) have been recalculated in the geographical reference frame although the angle between X_v sensor and the true North is small (around $0.37°$). In order to process the data, we have selected a 2 minute long interval approximately centered on the zero crossing of the Y record. A parabolic time function based upon 10 values at each end of the selected section has been substracted from the raw signal in order to extract the disturbance.

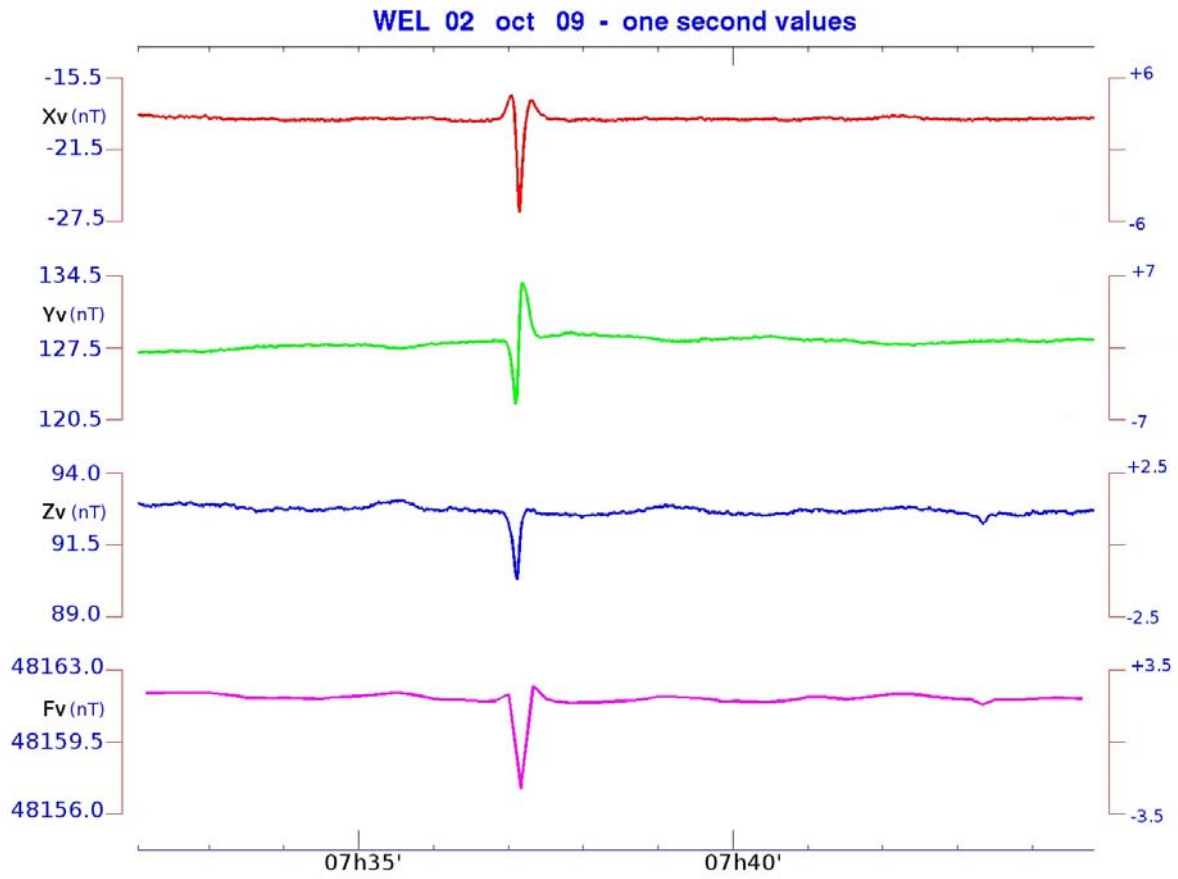

Figure 5: Disturbance recorded by the three sensors of the triaxial variometer (as well as by a scalar magnetometer (F_v).

4.1 Modelling an isolated disturbance

The parameters of the model are the components of the dipole and the velocity v (positive or negative) at the time t_0 of $s = 0$. In a preliminary version, we assumed that the dipole was parallel to the ambient field. It turned out that the theoretical signal, especially the Z component, was significantly larger than the observed one so that we quickly abandonned this assumption. The model being non-linear in v and t_0 , the estimation of the model parameters classically requires an initial estimate $(M^{(0)}, v^{(0)}, t_0^{(0)})$. This estimate is provided by a cross-correlation between each of the components recorded by the triaxial variometer and the corresponding modelled signal, calculated for a set of velocities ranging from $\pm 72 km/h$ to $\pm 9 km/h$ with $4.5 km/h$ sampling rate. The initial magnetic moment $M^{(0)}$ is estimated by the minimization of the difference between observed and expected signal obtained at $s = 0$. The cross correlation between two digital signals $S_1(n)$ and $S_2(n)$ is classically defined by:

$$R(\tau) = \sum_{n=N_1}^{N_2} S_1(n) S_2(n+\tau)$$

where τ is the shift between the two signals (see Figure 6). In order to compute the cross-correlation $R(\tau)$, we have used an adapted version of the function xcorr from the Signal Processing Matlab Toolbox. In our case, S_1 stands for one of the recorded components, and S_2 is the modelled signal, computed as described above.

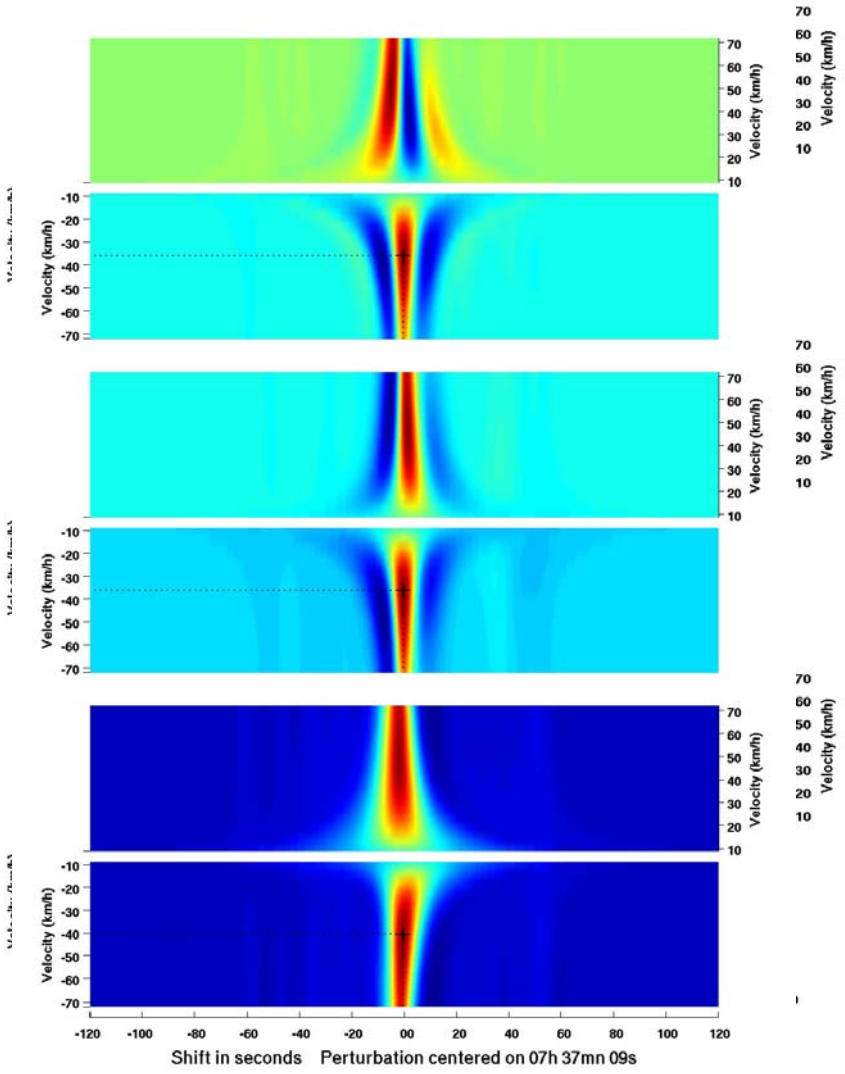

Figure 6. Cross-correlation between the selected piece of recorded disturbance (see Figure 5) and modelled signal computed for various negative and positive velocities. Blue zones: negative correlation; red zones: positive correlation. Two upper panels: X_V component; two middle panels: Y_v component; lower panels: Z_V component.

The maximum of positive correlation on Figure 6 provides a preliminary estimate of the time t_0 as well as an estimate of the velocity and direction of movement. Due to the shape of the Y disturbance, the estimates provided by this component are the most reliable and are used as initial guesses in the inversion process.

The estimation of the parameters M , t_0 , and v is refined further by a non-linear least-squares method using the Levenberg-Marquardt algorithm (Marquardt, 1963). The misfit to be minimised is written:

$$d^2 = \sum_{n=N_1}^{N_2} \left| B_v(t_n) - S_p(t_n) \right|^2$$

where the time interval defined by N_1 and N_2 is adjusted with respect to velocity in order to keep the curvilinear abscissae within the range of actual sampling. Note that the method requires the calculation of the first derivatives of S_p with respect to the parameters. In particular, in order to calculate the first derivatives with respect to the velocity, we need to know the derivatives of the trajectory with respect to the curvilinear abscissa. This is a by-product of the cubic spline approximation easily derived using the spspline Matlab function of the Spline Toolbox. Figure 7 left shows the fit of the model to the observed signal. We may note, as expected, the spurious effect of the inadequate sampling of the trajectory and may suspect that,

with a 0.5nT R.M.S., the model is not completely satisfying. The R.M.S is defined by:

$$R.M.S. = \left[\frac{d^2}{N_2 - N_1 + 1 - M} \right]^{1/2}$$

where M is the number of parameters in the model.

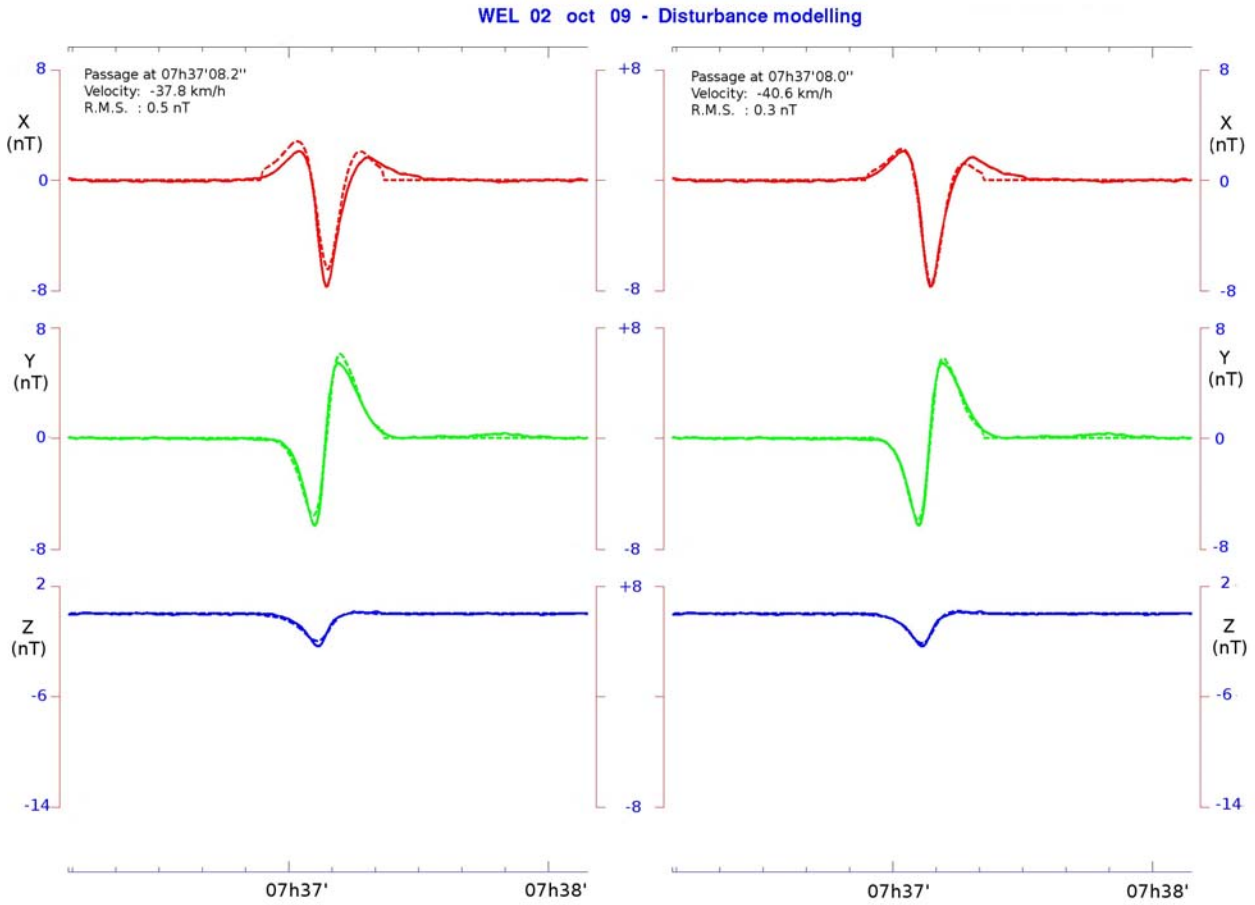

Figure 7. Left: Measured (solid lines) and modelled signal (dotted lines). Right: Same but considering a part of induction signal.

We have tried to improve the model by speculating the slight influence of an induction term due to the dipole moving at the surface of a conductive earth. Indeed, the time variation of S_g is given by:

$$\frac{\partial S_g}{\partial t} = \frac{\partial A}{\partial t} \cdot M$$

where A is the matrix explicited in Eq. (2). Neglecting the possible shift between primary and secondary signal, we have empirically incorporated the induction effect via a symmetric matrix α, which allows a small correlation between the three components of the primary disturbance field. S_p now written:

$$S_p = [(I + \alpha) \cdot A] \cdot M$$

where I is the 3x3 identity matrix. The elements of the matrix α are 6 parameters more to estimate. However, the solution is no longer unique with this additional refinement. We have circumvented the difficulty by the introduction of a minimum induction energy constraint. The misfit function takes now the form:

$$d^2 = \sum_{n=N_1}^{N_2} |B_v(t_n) - S_p(t_n)|^2 + \mu \sum_{n=N_1}^{N_2} |s_p(t_n)|^2 \quad (5)$$

Where $s_g = (\alpha \cdot A) \cdot M$ is the induced contribution. The subjective choice of the associated Lagrange multiplier μ allows us to control the order of magnitude of the induction effect. The larger μ is, the more reduced the induction effect is (this effect is negligeable for $\mu \backsim 10^5$). Typical values are $\backsim 10^{-3}$. Figure 7

right displays the improvement. The R.M.S. as defined by Eq. (4) drops from 0.5nT to 0.3nT. Assuming that the errors on B_v are independent, normally distributed random variables, we may implement a F-test in order to evaluate whether the two R.M.S. are significantly different. It turns out that the null hypothesis H_0 : $R.M.S_1 (= 0.5nT) = R.M.S._2 (= 0.3nT)$ against H_1 : $R.M.S_1 > R.M.S._2$ may be rejected with less than 5% risk of error.

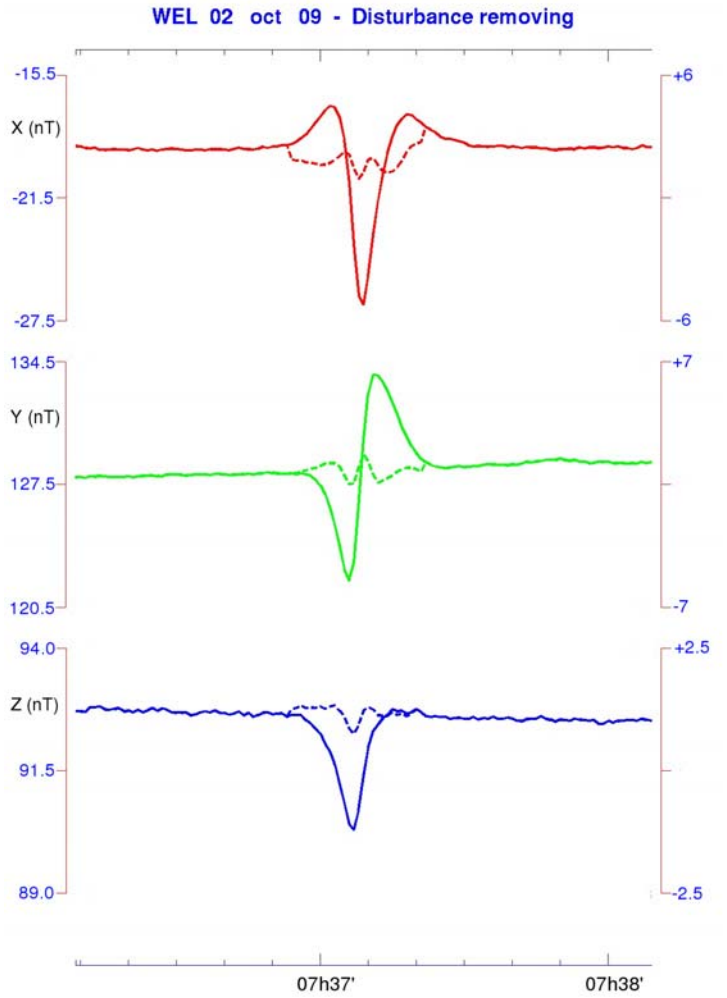

Figure 8. The magnetometer records disturbed by the passage of the vehicle, to be compared to the signal obtained after removal of the modelled disturbance displayed on Figure 7, right.

Figure 8 displays the shape of the magnetometer records after removal of the disturbance. Most of the residual disturbance, visible particularly on the X component, is due to the insufficient sampling of the road, uphill. Another small part of the residual disturbance probably arises from the non-constant actual velocity. Unfortunately, there is no mean with the available data to measure the acceleration of the disturbing vehicles. Finally, we may notice that the residuals have roughly the same shape as the disturbance itself however with a slight shift, which might be accounted for in a more elaborated model of the induction part.

4.2 Example with two successive disturbances

The following example is provided by the downwards passage of a bus followed some tens of seconds later by the upwards passage of a lorry. On Figure 9 we may notice that, in neither of the disturbances, the signal is as expected with a dipole roughly oriented in the direction of the ambient field. A several hours watch of the traffic has revealed that only buses and lorries give rise to a measurable signal. Cars and motorbikes are not detected.

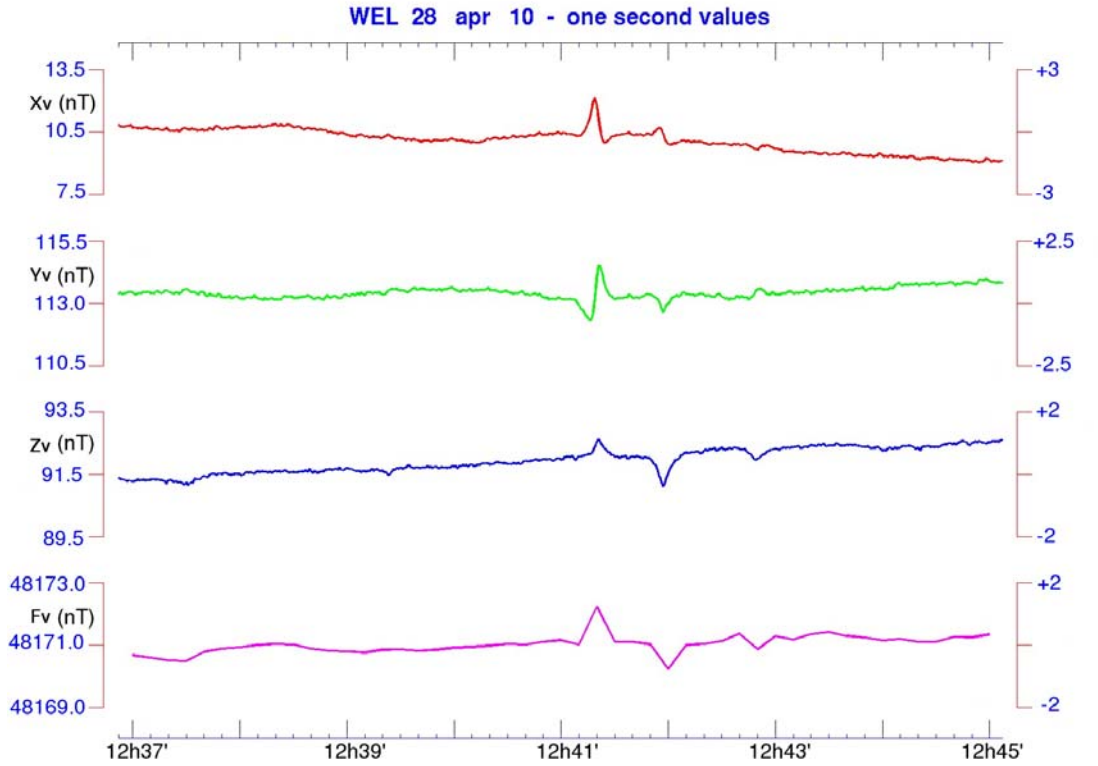

Figure 9. Disturbance produced by a bus, followed some tens of seconds later by a lorry.

Figure 10 shows that both disturbances are clearly identified by cross-correlation. However, the correlation is less accurate for the lorry due to the actual orientation of its equivalent dipole. The cross-correlations have been calculated with a dipole estimate based upon the disturbance due to the bus, which is obviously not appropriate for the disturbance due to the lorry. Further parameter estimations are restricted to the disturbance caused by the bus.

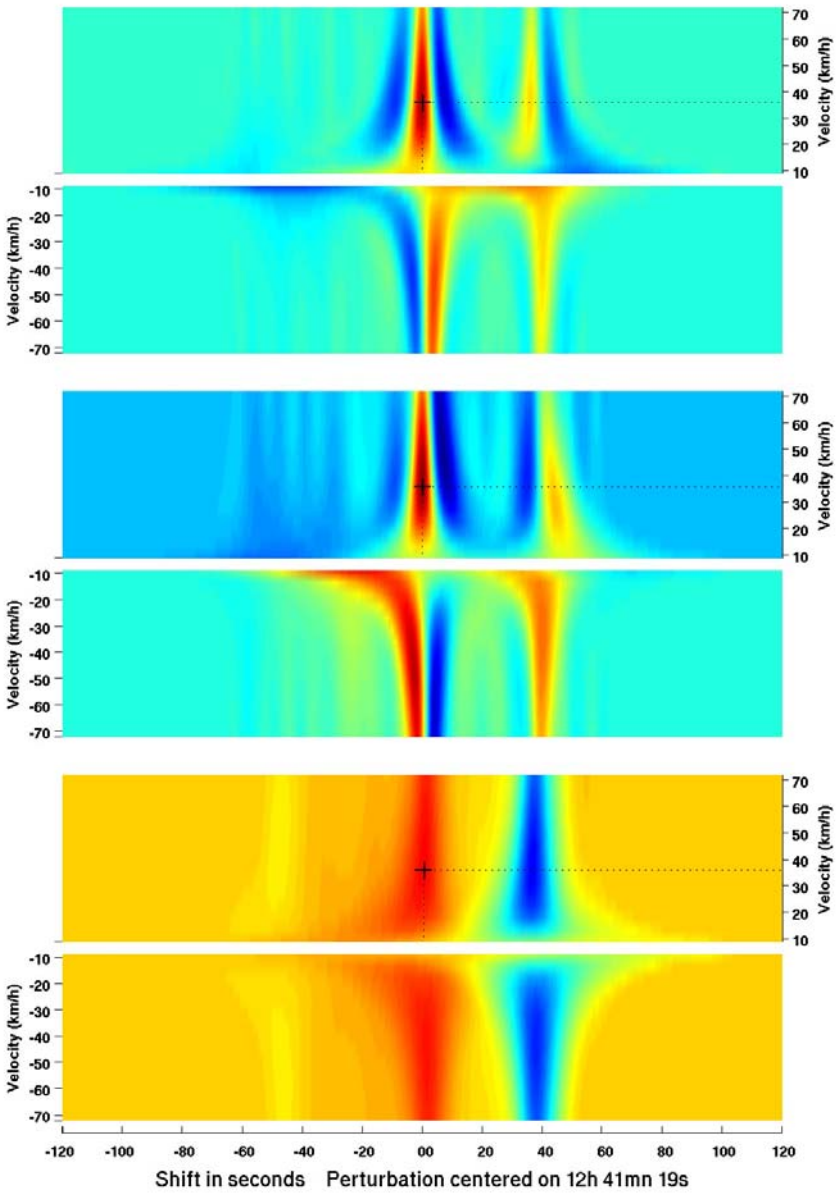

Figure 10. Same as Figure 6

Figure 11 left and right are the equivalent of Figure 7 right and Figure 8 respectively. We may notice on Figure 11 that the R.M.S. (provided by the model including some induction effect) is even better than in the previous example. This is partly due to the disturbance being weaker. On the other hand, the residuals displayed on Figure 11 right are very small, and in this example we are probably close to the limit of the disturbance removal that can be performed with this simple model.

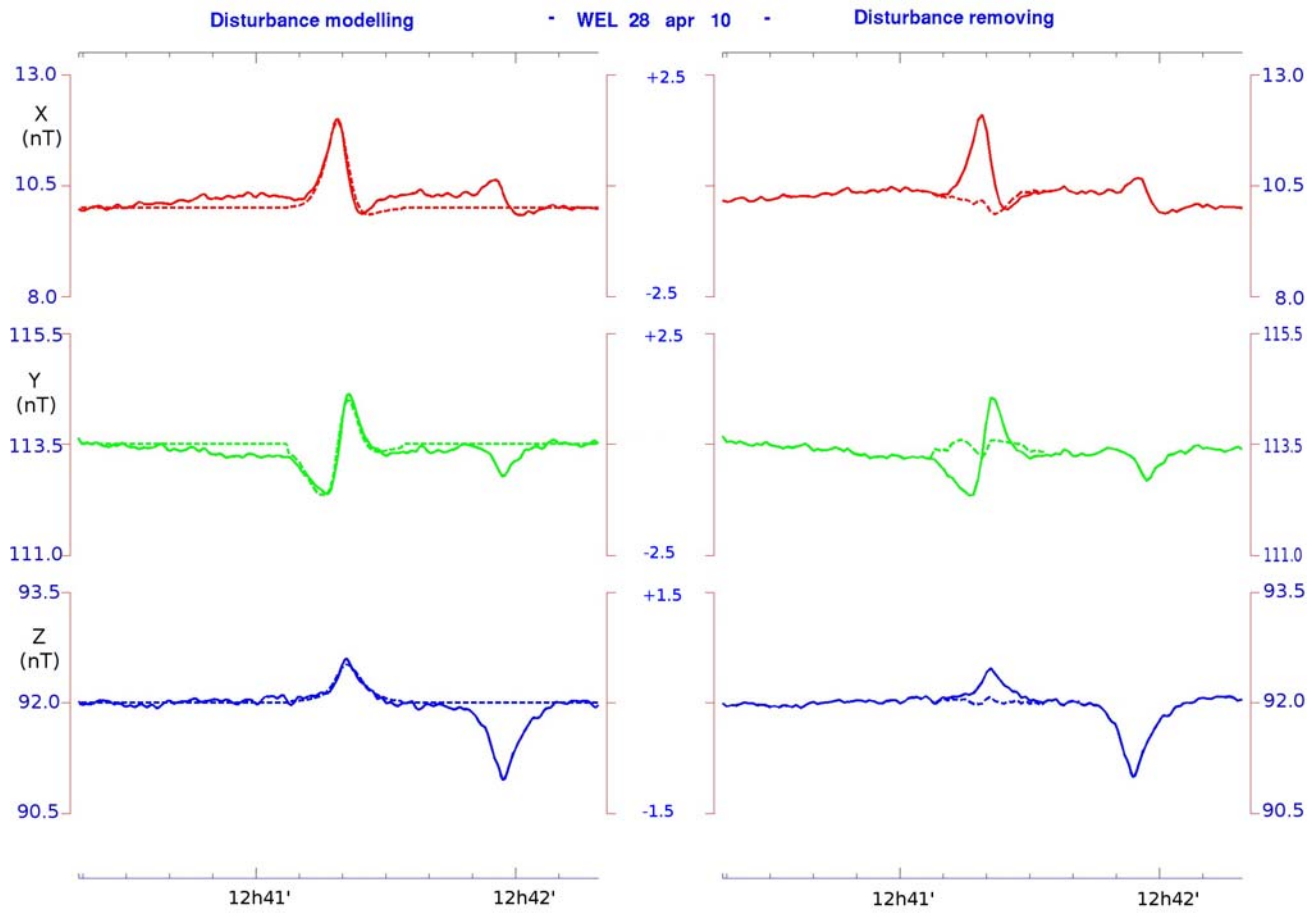

Figure 11. Left: same as Figure 7, right. Right: same as Figure 8.

5 CONCLUSION

It appears in the examples analysed in this work that one second records are a powerful tool for assessing the quality of a magnetic observatory. Indeed, in this case, whereas one minute records do not reveal any spurious influence, one second records show that the magnetic environment is far from perfect. In the present case, fortunately to some extent, the numerous disturbances observed on the one second records may be reasonably attributed to heavy vehicles, such as buses and lorries, passing on the road nearby. These vehicles are assumed to be disturbing field sources due to their magnetization. A simple dipolar approximation seems to work well and be appropriate to identify the main properties of the sources, such as the dipolar moment, the velocity, and direction of movement. There are however two complications:

1. the dipole is not parallel to the ambiant field;
2. the model fits better the recorded disturbance if a small induction contribution is incorporated.

The plausibility of this latter assumption would need further investigations in order to estimate its order of magnitude based upon physical assumptions and, in particular, on some knowledge of the ground conductivity.
The automatic removal of the disturbances is another issue which has been left aside, all the more as the station has not the status of a registered observatory. However, regarding this specific disturbance, an automatic processing might be easily imagined, at least in the studies where one second data would be necessary.

6 ACKNOWLEDGEMENTS

We acknowledge gratefully the collaboration of J. Durand, who performed the GPS measurements along the section of road and critically read the paper, and that of D. Boulanger, who provided the GPS equipment and processed the data. The authors would like to thank the anonymous reviewer for his constructive comments.

7 REFERENCES

Clark, T.D.G., Carruthers, A., & Carrigan, J.G. (1994) A discussion on the problem of mains interference at magnetic observatories. *Proc. VIth Workshop on geomagnetic observatory instruments, data acquisition and processing* (pp. 219–225). Dourbes, Belgium.

Fotzé, M., Chambodut, A., Bernard, A., & Schott, J.J. (2007) New acquisition systems in French austral magnetic observatories. *Proc. IUGG XXIVth General Assembly.* Perugia, Italy.

Hejda, P. & Horacek, J. (2001) On the industrial noise of the geomagnetic field in Prague. *Contributions to Geophysics and Geodesy*, 31, pp. 159-161.

Marquardt, D.W. (1963) An algorithm for least-squares estimation of nonlinear parameters. *J. Soc. Indust. Appl. Math.*, 11, pp. 431–441.

Okawa, T., Tokumoto, T., Nakajima, S., Owada, T., Toya, T., Muromatsu, F., Kumasaka, N., & Koike, T. (2007) Development of artificial geomagnetic disturbances monitoring system. *Publs. Inst. Geophys. Pol. Acad. Sc.*, C-99(398), pp. 183-188.